

## Characterization and prediction of microporosity defect in HASTELLOY G30.

O.BEN LENDA<sup>1\*</sup>, F.SABIR<sup>1</sup>, A.AMRI<sup>1,2</sup>, L.ZERROUK<sup>1</sup>, A.IBNLFASSI<sup>2</sup> AND E.SAAD<sup>1</sup>.

1. Laboratory of Physical-Chemistry of Process and Materials, University Hassan 1st, FSTS, 577 SETTAT, Morocco.

2. Laboratory of Environmental Sciences and Development, University Hassan 1st, FSTS, 577 SETTAT, Morocco.

\* e-mail : o.benlenda@uhp.ac.ma

### Abstract :

In this paper, we analyzed the Hastelloy G30 by some techniques of characterization in order to interpret the results obtained through a computer simulation of the filling and the solidification of the casting. The design of the filling system, the riser and the plate was carried out by the software SOLIDWORKS. The thermo-physical properties of the alloy, the simulation of the filling and solidification of the casting was performed by the software ProCast. The software JMATPRO was used to confirm the thermo-physical properties of the alloy. The validation of numerical results was done by the following experimental techniques : optical microscopy, hardness test and X-ray diffraction. The numerical and experimental results showed the appearance of a porosity caused by a non-uniform solidification of the casting, leading to embrittlement of the alloy.

**Keywords :** *Porosity, Hastelloy G30, ProCast, Optical Microscopy, X-Ray Diffraction.*

### 1. Introduction :

In the 1990s, there has been renewed interest in the ability to predict the formation of defects in single-crystal, investment-cast Ni-based superalloys [1 – 6]. Alloy casting solidification processes involve many physical phenomena such as chemistry variation, phase transformation, heat transfer, fluid flow, microstructure evolution, and mechanical stress [7].

The first model for porosity prediction was developed by Kubo and Pehlke in two-dimensions (2D) [8] and was based on the relationship between the fraction of porosity and local pressure. Lee and Hunt [9] simulated the growth of pores due to hydrogen diffusion in Al-Cu alloys using a 2D continuum diffusion model, combined with a stochastic model of pore nucleation. Although the model did not include the effect of pressure drop due to shrinkage, it showed a good correlation with in situ observations of pore growth. Later, Lee and al. [10] developed a multi-scale model of solidification in Al-Si-Cu alloys, including microsegregation and microporosity. ProCast was used to solve the energy, momentum, and continuity equations to determine the temperature and pressure evolution with time. This

information was coupled to a mesoscale model for microstructural development. Carlson and al. proposed a volume-averaged model for finite rate diffusion of hydrogen in Al alloys [11]. They coupled the calculation of the micro/macroscale gas species transport in the melt with a model for the feeding, flow, and pressure field. This was the first work considering hydrogen diffusion in the growth of pores for three-dimensional (3D) calculations. Pequet and al. developed a 3D microporosity model based on the solution of Darcy's equation and microsegregation of gas [12]. The model coupled microporosity with macroporosity and pipe-shrinkage predictions in a coherent way, with appropriate boundary conditions. Later, this approach was improved by developing a porosity model for multi-gas systems in multi-component alloys, including a realistic model for pore pinching [13].

The quality of alloys is commonly affected by various internal defects like porosity. The aim of this work is to analyze the alloy Hastelloy G30 by techniques of characterization and to interpret the results obtained through a simulation of its solidification.

### 2. Materials :

#### 2.1. Composition of the alloy G30 :

The superalloy Hastelloy G30 is an alloy with a high proportion of nickel, characterized by a high corrosion resistance in environments containing extra oxidizing acids. The alloy consists essentially of 43% of nickel with a proportion of chromium which varies from 28 to 31.5% and from 13 to 17% for iron

#### 2.2. Procedure of simulation :

The design in 3 dimensions of the plate, the riser and the filling system was carried out by the software SolidWorks. The determination of the thermo-physical properties of the alloy, mesh and simulation of filling and solidification of the casting was carried out by the software ProCast. The confirmation of the thermo-physical properties of the alloy was done by the software JMatPro.

The parameters used in the simulation : a filing time of 10 seconds, a casting temperature of 1320 °C and a preheating temperature of the mold of 1000 °C.

### 2.3. Microscopic study :

The metallographer used is Optika B-383MET type. The microscopic study require mechanical polishing followed by chemical etching. In the case of the alloy G30, we use aqua regia and the immersion time is between 5 and 60 seconds [14].

### 2.4. X-ray diffraction :

Diffraction data were collected at room temperature on a D2 PHASER diffractometer, with the Bragg–Brentano geometry, using  $\text{CuK}\alpha$  radiation ( $\lambda=1.5418 \text{ \AA}$ ) with 40KV and 30 mA. The patterns were scanned through steps of  $0.01^\circ$  in the  $2\theta$  range  $15\text{--}100^\circ$ .

### 2.5. Hardness measurement :

Hardness tests are performed using a durometer WILSON type. The method used is ROCKWELL C.

## 3. Results and Discussions

### 3.1. Thermophysical properties of the alloy :

The figure 1 shows a comparison between the physical properties of the alloy Hastelloy G30 determined by the softwares ProCast and JMatPro. We observed that the difference between the curves provided by the two softwares is acceptable.

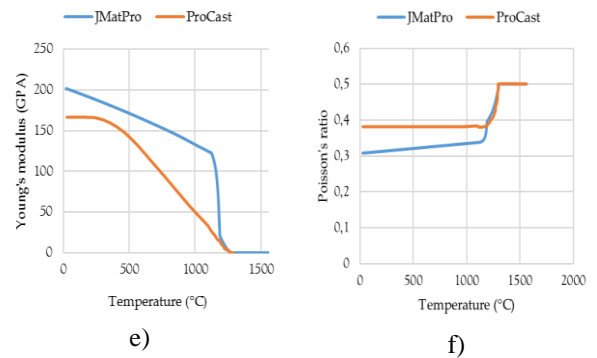
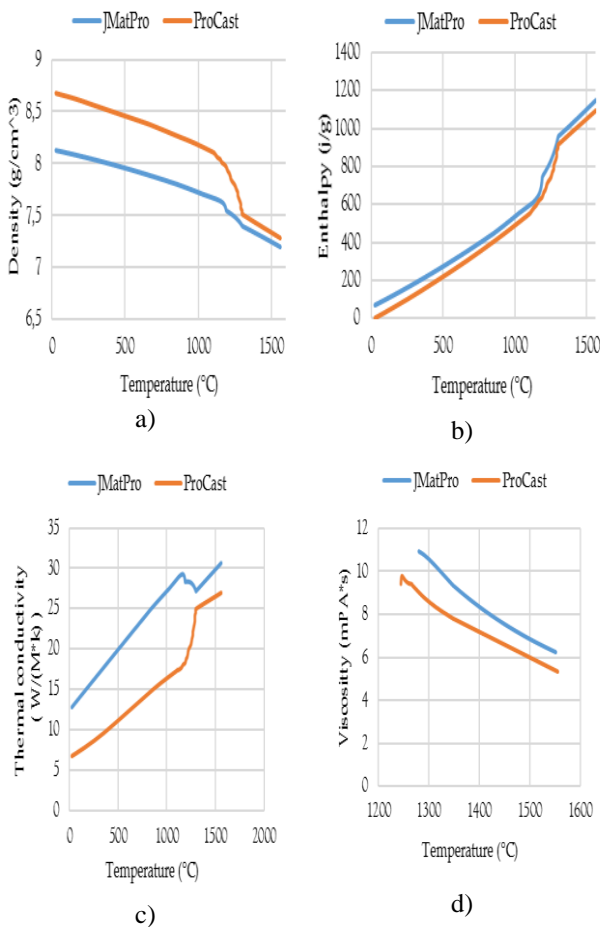


Figure 1 : thermophysical properties of the alloy G30 : a) Density, b) enthalpy, c) thermal conductivity, d) viscosity, e) Young's Modulus and f) Poisson's Ratio

### 3.2. Results of filling and solidification numerical of the alloy:

The figure 2 shows the temperature field of the plate after 12 seconds. We noted that we have a maximum of temperature at the center of the alloy ; this temperature is higher than the liquidus, while the temperature at the corners is lower than the solidus.

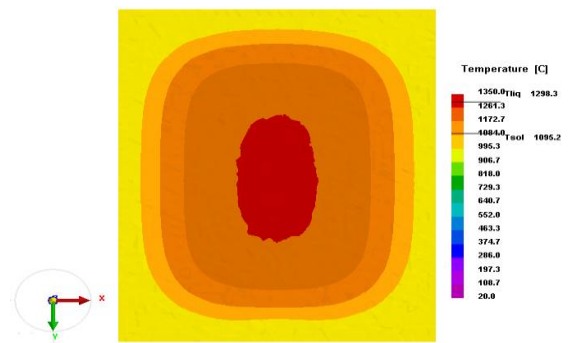


Figure 2 : the temperature field of the plate after 12 seconds.

The Figure 3 shows the fraction of solid of the plate after 13 seconds. We noted that during solidification, a fraction of the liquid is trapped in the center of the alloy. The liquid islands form the potential defects since no liquid feeding metal can be introduced into these areas during the process of solidification.

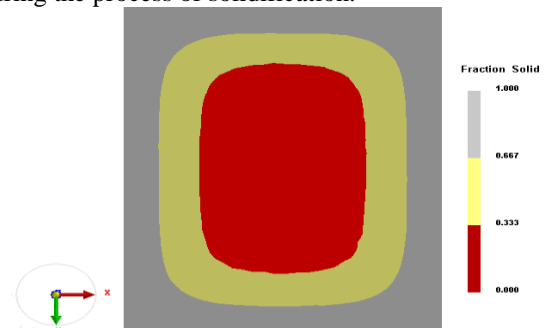


Figure 3 : the fraction of solid of the plate after 13 seconds.

Figure 4 shows the prediction of the porosity of the plate after solidification. We observed that the predicted porosity in the center of the plate is between 0.44 and 1.78%, while the rest of the plate is "homogeneous".

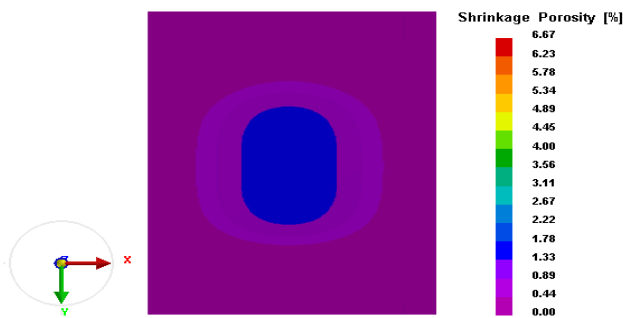


Figure 4 : Porosity of the plate after solidification

### 3.3. Microscopic study :

The figure 5 shows the micrographs of the center of the alloy. We observed the appearance of pores in the center of the plate. In other areas (four corners), we saw just the austenitic matrix with precipitates.

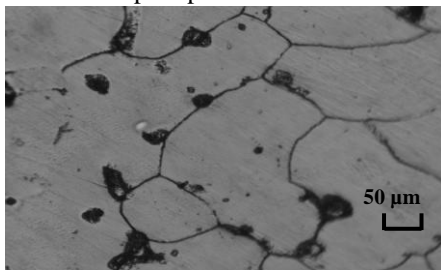


Figure 5 : Micrographs of the center of the alloy.

### 3.4. X-ray diffraction :

According to the peak positions of the spectrum, the alloy HASTELLOY G30 has a face-centered cubic structure characterized by crystallographic planes of families : (110), (200), (220), (311) et (222).

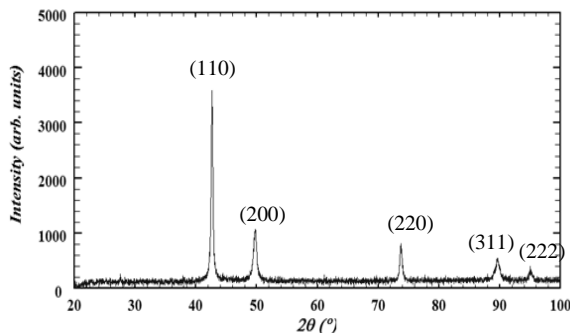


Figure 6 : X-ray diffraction spectrum of the alloy G30

### 3.5. Hardness measurement :

We measured the hardness of the alloy G30 in the four corners and in the center after elaboration. We have noticed, a hardness of 32 HRC at the four corners, it is higher than the center of the alloy which is 29 HRC.

## 4. CONCLUSION :

We did numerical and experimental study of filling and solidification of the alloy Hastelloy G30. The X-Ray Diffraction revealed that the alloy crystallizes in face-centered cubic structure. Optical microscopy revealed the presence of pores in the center of the alloy where a decrease in hardness was noted compared to the corners

of the plate. We note also, the precipitation of carbides rich in chromium in the matrix determined by M.E.B. The numerical results showed that a fraction of the liquid is trapped in the center of the plate during cooling. Therefore, the solidification of the alloy G30 is done with a non-uniform manner and that leads to a shrinkage porosity which negatively influence the quality of the alloy.

## References :

- [1] K.O. Yu, and all , *Solidification modeling of single-crystal investment castings*, AFS Trans., 417-28.
- [2] K.O. Yu and all, *Finite-element thermal modeling of casting microstructures and defects*, JOM, 21 - 25.
- [3] J.S. Tu and all , *The application of defect maps in the process modeling of single-crystal investment casting*, JOM, 26 -28.
- [4] A.L. Purvis and all, *characteristics for solidification in single-crystal, investment-cast superalloys*, JOM, 38 – 41.
- [5] A.L. Purvis and all, *Importance of thermal parameters as vector components during solidification modeling of single-crystal investment casting*, AFS Trans., 637 - 44.
- [6] T.M. Pollock and all , *The breakdown of single-crystal solidification in high refractory nickel-base alloys*, Metall. Mater. Trans. A, 1081-94
- [7] J. Guo and M. Samonds, *Casting Design and Performance*, Materials Park OH: ASM International, United States of America, 2009.
- [8] Kubo K. and all., *Mathematical modeling of porosity formation in solidification*, Mater Trans B, 359–366.
- [9] Lee PD and all, *Hydrogen porosity in directionally solidified aluminium copper alloys: a mathematical model*, Acta Mater, 1383–1398.
- [10] Lee PD and all, *Multiscale modeling of solidification microstructures, including microsegregation and microporosity, in an Al-Si-Cu alloy*, Mater Sci and Eng A, 57–65.
- [11] Carlson KD and all., *Modeling the effect of finite-rate hydrogen diffusion on porosity formation in aluminum alloys*, Metall Mater Trans B, 541–555.
- [12] Pequet C and all. , *Modeling of microporosity, macroporosity, and pipe-shrinkage formation during the solidification of alloys using a mushy-zone refinement method: applications to aluminum alloys*, Metall Mater Trans A, 2095–2106.
- [13] Couturier G and all., *Effect of volatile elements on porosity formation in solidifying alloys*, Model Simul Mater Sci Eng, 253–271.
- [14] Asm International Handbook Committee, *ASM Handbook: Volume 9 : Metallography and Microstructures*, Materials Park OH: ASM International, United States of America, 2004.